

Protective effect of MAPK signaling pathway mediated by ITGB3 gene silencing on myocardial ischemia-reperfusion injury in mice and its mechanism

M.-C. WANG, D. WANG, Y.-H. LU, Z.-H. LI, H.-Y. JING

Department of Cardiology (v), Zhengzhou Central Hospital Affiliated to Zhengzhou University, Zhengzhou, Henan Province, P.R. China

Abstract. – **OBJECTIVE:** To explore the effect of integrin $\beta 3$ (ITGB3) gene silencing mediated mitogen-activated protein kinase (MAPK) signaling pathway on myocardial ischemia-reperfusion injury (MIRI) in mice.

MATERIALS AND METHODS: MIRI mice model was established, and myocardial tissues of MIRI mice and sham operation group mice were extracted. Hematoxylin-Eosin (HE) staining was used to observe the pathological changes of myocardial tissue; terminal deoxynucleotidyl transferase-mediated dUTP-biotin nick end labeling (TUNEL) staining was used to detect the apoptosis of myocardial cells; ELISA method was used to detect the levels of interleukin (IL)-1, IL-6, and tumor necrosis factor (TNF)- α in the two groups. The infarct size was measured by TTC staining. Myocardial cells of MIRI model mice were isolated and cultured, and then grouped and transfected. The cells were transfected with the grouping of MIRI group, negative control (NC) group, MAPK signal pathway agonist Anisomycin group, MAPK signal pathway inhibitor SB203580 group, ITGB3-siRNA group, SB203580 + ITGB3-siRNA group. Real-time quantitative polymerase chain reaction (qRT-PCR) and Western blot were used to detect the mRNA and protein expressions of ITGB3, p38MAPK/p-p38MAPK, GSK-3 β /p-GSK-3 β , Cx43/p-Cx43, pro-apoptotic factor Bax and anti-apoptotic factor Bcl-2. 3-(4,5)-dimethylthiazolide (-z-y1)-3,5-di-phenyltetrazolium bromide (MTT) assay was used to detect cell proliferation and flow cytometry to detect cell apoptosis.

RESULTS: The expression of ITGB3 in myocardial tissue of MIRI mice was significantly higher than that of sham operated mice ($p < 0.05$). Compared with the sham operation group, the apoptosis rate of myocardial cells in MIRI group was significantly increased, the expression levels of IL-1, IL-6 and TNF- α were significantly increased, and the myocardial infarction area was significantly increased (all $p < 0.05$). Compared with MIRI and NC groups, ITGB3 mRNA

and protein expression levels in ITGB3-siRNA group and SB203580 + ITGB3-siRNA group were significantly decreased (all $p < 0.05$), but no significant change was found in Anisomycin group and SB203580 group ($p > 0.05$). Furthermore, ITGB3-siRNA group and Anisomycin group had markedly decreased mRNA and protein expressions of ITGB3 and Bax, increased mRNA and protein expressions of p38MAPK/p-p38MAPK, GSK-3 β /p-GSK-3 β , Cx43/p-Cx43 and Bcl-2, as well as increased cell proliferation and decreased cell apoptosis (all $p < 0.05$); SB203580 group indicated an opposite result with Anisomycin group; while SB203580 + ITGB3-siRNA revealed none significant statistical difference. In addition, compared with ITGB3-siRNA group, SB203580 + ITGB3-siRNA group showed significantly upregulated mRNA and protein expressions of Bax, downregulated mRNA and protein expressions of p38MAPK/p-p38MAPK, GSK-3 β /p-GSK-3 β , Cx43/p-Cx43 and Bcl-2, as well as decreased cell proliferation and increased cell apoptosis (all $p < 0.05$).

CONCLUSIONS: Silencing ITGB3 gene expression can promote the activation of MAPK signaling pathway, elevate the phosphorylation of GSK-3 β and Cx43 in the downstream, promote the proliferation of mouse myocardial cells, inhibit myocardial cell apoptosis and inflammatory reaction, and thus have protective effect on MIRI in mice.

Key Words:

ITGB3, Gene silencing, MAPK signaling pathway, Myocardial ischemia-reperfusion injury, Proliferation, Apoptosis.

Introduction

Cardiovascular disease is still the leading cause of death and produces the heaviest burden in the world¹. As for the occurrence of

myocardial ischemia-reperfusion injury (MIRI), myocardial reperfusion may be accompanied by microvascular injury, capillary endothelial cell and myocardial cell swelling frequently, leading to the so-called “no-reflow”²⁻⁴. More importantly, reperfusion after severe ischemia is considered as a “double-edged sword”⁵. It can save the damaged myocardium, reduce the size of myocardial infarction, protect left ventricular systolic function, etc.^{6,7}. It may, however, cause further myocardial damage, namely MIRI, which seriously weakens the therapeutic effect in the clinical practice⁸. Its mechanism has been discovered to be closely related to inflammation, oxidative stress and apoptosis, etc.⁹. In this regard, intervention on inflammation or reduction of myocardial cell apoptosis and other therapeutic approaches are of great significance in the prevention and treatment of MIRI.

A large number of studies have used animal models of coronary artery occlusion and reperfusion to treat MIRI¹⁰⁻¹². Various endogenous and pharmacological methods have been adopted to reduce MIRI, including ischemic preconditioning, ischemic postconditioning, as well as drug preconditioning and drug postconditioning^{13,14}. Both pretreatment and postconditioning can exert a cardioprotective role by activating a series of survival promoting signal transduction pathways in the early stage of reperfusion¹⁵. Among them, the inhibition of mitogen-activated protein kinase (MAPK) signaling pathway is recognized to play a role in myocardial protection¹⁶. p38 is one of the most important members of MAPK family, which can regulate intracellular responses (such as cell stress, inflammatory response, cell cycle, apoptosis, differentiation and aging) in a variety of physiological/pathological processes^{17,18}. Meanwhile, GSK-3 β is a serine/threonine kinase, which not only regulates glucose metabolism, but also participates in cell proliferation and other signaling pathways¹⁹. As a key regulator of MAPK signaling pathway, dysfunction of GSK-3 β will lead to a variety of physiological disorders²⁰. It is a common pathway of many signaling molecules, which plays an important role in the conduction of myocardial protection signals²¹. The increase of GSK-3 β phosphorylation level, that is, the decrease of its activity, is an important part in exerting the role of myocardial protection^{22,23}. In addition, Cx43 is a major protein in gap junction channel of mammalian myocardium²⁴. It involves significantly in cell volume regulation, ATP release and metabolites release through its

unconnected half channel²⁵. It is easy to degrade during myocardial ischemia-reperfusion. It has been found that ischemic preconditioning can maintain the level of Cx43, maintain the gap junction structure, and hence reduce the occurrence of arrhythmia, the diffusion of harmful substances, and the damage of myocardial cells^{26,27}. The above interpretation supports that regulation in the MAPK signaling pathway can generate a protective role in MIRI through proper mediation.

Furthermore, integrins are cell surface molecules, which are transmembrane protein receptors composed of α and β subunits in the form of non-covalent bonds, which mediate the adhesion of cell-cell and cell-extracellular matrix (ECM)²⁸. Integrin has two-way signal transduction function because of its special transmembrane structure. At present, eighteen α subunits and eight β subunits have been found, which can form 24 hetero-dimers that are distributed in different tissues and organs of the body and play their respective biological functions²⁹. The mutation or abnormal expression of integrin is considered to be related to the occurrence and metastasis of various diseases³⁰. More importantly, integrin is also expressed in cardiovascular system, vascular cells, myocardial cells and non-myocardial cells. It is the most important molecule that mediates the interaction between cells and ECM. It can recognize and bind the corresponding ligands in ECM, provide attachment points for cell adhesion, and mediate the phosphorylation level and activity of relevant proteins in the downstream signal transduction pathway. Accordingly, as a molecule involved in adhesion and cell signal transduction, integrin plays an important role in cardiac muscle fiber formation, organ formation and internal stability of normal myocardial function during cardiac development. Among them, integrin β 3 (ITGB3) is a member of β subunit that is expressed in different tissues of the body, participates in a variety of biological processes and plays different physiological functions³¹. ITGB3 can change the normal biological process of endothelial cells by interacting with fibronectin of ECM, can also affect platelet formation and involve in coagulation process according to its salt bridge structure^{31,32}. Meanwhile, interference with ITGB3 can affect cell adhesion and migration, or tumor cell metastasis by promoting the development of osteoclasts³³. Additionally, it can affect the formation of stem cells by stimulating transcription factors into the nucleus and can also recruit small molecules to form complex to

participate in the drug tolerance of cells³⁴. But there is a limited research concerning the role of ITGB3 in MIRI.

Consequently, in accordance with our previous searching that ITGB3 is a relevant factor of MAPK signaling pathway, the present study was carried out to explore effect of ITGB3 gene expression and MAPK signaling pathway on an established mouse model of MIRI and myocardial cells with certain interventions, with the aim to broaden understanding in the molecular therapy of cardiovascular diseases.

Materials and Methods

Objects of Study

In this experiment, healthy C57BL/6J mice (half male and half female) aged 20 weeks were used, weighing 25-35 g. During the experiment, the animals were raised in the SPF rodent experimental area of the experimental animal center. The animals were raised by special personnel and artificially illuminated, which were fed with ordinary feed and free water for 12 h (8 a.m.; 8 p.m.) in the daytime and at night respectively. The indoor temperature was 18-25°C, and the relative humidity was 40-70%. All experiments were performed in accordance with the Guide for Care and Use of Laboratory Animals (NIH Pub. No. 85-23, revised 1996). Experimental procedures performed in our research has been reviewed and approved by the Local Animal Ethics Committee of our Hospital of Zhengzhou Central Hospital Affiliated to Zhengzhou University.

Establishment of a Mouse Model of MIRI

There were 30 wild-type C57BL/6J male mice, 20 of them were used to establish MIRI model (experimental group), and 10 were included in the sham operation group as control. After weighing the mice, ketamine (90 mg/kg) combined with diazepam (5 mg/kg) was injected intraperitoneally. After the anesthesia was confirmed to be successful according to the muscle tension of mice limbs, the mice were fixed on the operating table in the supine position. After disinfection of the anterior cervical area, median skin of the mouse neck was cut off, the tissue was separated, and tracheal intubation was conducted along the direction of trachea. The tracheal tube was connected with a ventilator, and the parameters were set as follows: tidal volume of 1.0 ml/100g body weight, frequency of 120 times/min, and inhalation/ex-

halation ratio of 1:1.5. The chest was exposed in the fourth intercostal space on the left edge of sternum to peel off the pericardium and expose the heart. Between the left auricular appendix and the conus arteriosus, a small, pink, translucent left coronary artery (LCA) can be observed under the myocardial layer. A small non-invasive small round needle of 8-0 silk thread was used to inject the needle at LCA. The depth of the needle was controlled at 1 mm and the width was about 2 mm. The use of polyethylene tube could induce the compression of blood vessels by pushing the vessels, resulting in myocardial ischemia. After 45 min, the silk thread was released to restore coronary blood flow. In the sham operation group, LCA was only threaded without ligation. The local color changes of left ventricular anterior wall before and after ligation were observed by naked eyes to judge whether the model was successful or not. When the ligation was successful, the local area of the left ventricle was immediately pale, with the observation of swelling, cyanosis and decreased contractility subsequently. Within seconds after successful reperfusion, the left ventricular region was rapidly congested, and the color of ischemic myocardium changed from dark red to bright red.

In terms of sample collection, after ischemia for 45 min and reperfusion for 4 h, a volume of 5 ml of 2% Evans blue was injected into the external jugular vein. After the heart surface turned blue, the mice were killed by injecting 10% potassium chloride. After cardiac arrest, the heart was taken, and the auricle and surrounding tissues were cut off quickly. The residual blood in the ventricle was washed out in phosphate buffer solution at 4°C. The heart was frozen in -70°C refrigerator for 30 min. Then, the cardiac tissue with a thickness of 2 mm at the apex of the heart was cut, and 10% formaldehyde solution was used for fixation to prepare paraffin embedded sections. Furthermore, from the apex to the bottom of the heart, the long axis of the heart was perpendicular. Except for the apex of the heart, other cardiac tissues were cut to prepare myocardial sections about 1 mm thick, which were used for the determination of myocardial ischemia area and myocardial infarction area and numbered in sequence.

Hematoxylin-Eosin (HE) Staining

In the process of HE staining, hematoxylin staining solution is alkaline, which mainly makes the chromatin and nucleic acid in the nucleus

appear purple blue; eosin is an acid dye, which mainly makes the components in cytoplasm and extracellular matrix red. On the basis of this principle, this experiment was performed to observe the pathological change of normal and ischemic necrotic myocardial cells. As for the specific steps, the frozen sections of 5 μm in thickness were incubated in a baking oven at 60°C for 2 h. In the next step of hematoxylin staining, there was a need to observe whether there was a layer of membranous solid on the surface of hematoxylin staining solution prior to experiment. If so, the solution shall be filtered, otherwise the staining effect would be affected. If not, the hematoxylin staining solution was directly added to the slices, stained for 2 min, and then washed with ultra-pure water for 2 min to remove the staining solution that did not bind to cells. For differentiation, 1% hydrochloric acid ethanol was used to differentiate for 7 s, followed by washing with ultra-pure water for 3 min. The 1% ammonia was used in the next step of re-bluening for 30 s. As for eosin staining, 1% eosin was used to stain the cells for 2 min, followed by washing with ultra-pure water for 5 s. After drying at room temperature, the normal and necrotic myocardial cells could be clearly identified according to the cell status by using neutral resin sealing and observing under the microscope (100 \times and 400 \times).

***Terminal Deoxynucleotidyl
Transferase-Mediated dUTP-Biotin
Nick end Labeling (TUNEL) Staining***

The tissue blocks were fixed, embedded in paraffin and sectioned at 4 μm . The slices were routinely dewaxed with xylene and washed with alcohol at gradient concentrations (xylene I for 5 min, xylene II for 5 min, 100% alcohol for 2 min, 95% alcohol for 1 min, and 80% alcohol for 1 min, 75% alcohol for 1 min), and then distilled water washing for 2 min. The slides were then treated by fresh 3% H₂O₂ for 10 min, followed by washing with distilled water for 2 min ($\times 3$ times). The specimens were digested with 0.01 M TBS freshly diluted protein K (1:200) at 37 °C for 10-15 min and washed with 0.01M Tris Buffered saline (TBS) for 2 min ($\times 3$ times). Labeling buffer (20 μL /slide) was added to the specimen to keep the slices moist. An amount of 1 μL TDT and 1 μL DIG-d-UTP was collected separately for each slide and added into 1 μL labeling buffer to mix well. After above processing, the blocking solution (50 μL /slide) was added and reacted at room temperature for 30 min, followed by shaking off

the sealing liquid without washing. The diluted biotinylated anti-digoxin antibody (1:100; 1 ml antibody dilution + 10 μL biotin anti-digoxin antibody) was added into the specimen (50 μL /slide), which were reacted in wet box at 37°C for 30 min. After washing twice with 0.01 M TBS (2 min each), 10 μL SABC diluted with 1 ml antibody diluent was added into the specimen (50 μL /slide), which were reacted at 37°C for 30 min. After another 0.01 M TBS washing (5 min $\times 4$ times), DAB development was performed for 30 min, followed by distilled water washing, mild re-staining with hematoxylin, dehydration, transparent processing, sealing, and observation under microscope. In terms of the result determination, those with brown granules in the nucleus were positive cells, namely apoptotic cells. Each section was observed under light microscope, and 10 visual fields were randomly selected to calculate the average number of positive cells in the cells, which was the apoptosis index (AI).

***2, 3, 5-triphenyltetrazolium Chloride
(TTC) Staining***

The tissue sections collected from the above animal specimens were put into the phosphate buffer solution of 1% TTC and incubated in the dark at 37°C for 15 min. The incubated myocardial slices were immersed in 10% formaldehyde solution for 24 h to enhance the contrast between stained and unstained regions. The myocardial slices were placed evenly with the same orientation of each section. Digital camera was used to adjust the uniform focal length under bright light. The pictures showed that the blue area was normal myocardium, (light) red was ischemic viable myocardium, (gray) white was necrotic myocardium. The area of infarct size (IS), ischemic survival area (ischemia) and left ventricle (LV) were measured by Image J software (NIH, Bethesda, MD, USA), in which area at risk (AAR) was equal to IS + necrotic zone. Results were expressed as the proportion as follows: infarct area = IS/AAR.

qRT-PCR

UNIQ-10 column-type TRIzol total RNA extraction kit was used for RNA extraction. The first strand of cDNA was synthesized by reverse transcription. The cDNA kit and RNA samples were thawed on ice in advance. The corresponding RNA loading volume was calculated according to 200 ng RNA loading volume, and the reverse transcription system was prepared. After the system was gently mixed, the conditions for

reverse transcription were as follows: incubation at 25 °C for 10 min, 50°C for 30 min, and 85°C for 5 min. After that, 1 µL E. coli RNase H was added and incubated at 37°C for 20 min and the samples were stored in a refrigerator at -20°C. Using SYBR fluorescent dye method, GAPDH was used as internal reference gene for the detection of the mRNA expression levels of ITGB3, interleukin (IL)-1, IL-6, and tumor necrosis factor (TNF)- α , Bcl-2 and Bax. The primers for real-time quantitative PCR were synthesized by Shanghai Generay Biotech Co., Ltd. The power up™ SYBR™ green master mix qPCR kit, DEPC, primers and cDNA samples were thawed on ice in advance. qPCR reaction system included 5µL power up SYBR green master mix (2×), 1µL forward primer (5 µM), 1 µL reverse primer (5 µM), 2 µL cDNA, and 1 µL DEPC-treated water. The reaction conditions using ABI 7500 were as follows: UDG enzyme activation at 95°C for 2 min; pre-denaturation at 50°C for 2 min; denaturation at 95°C for 15 s; and annealing at 60°C for 1 min, with a total of 40 cycles. The dissolution curve was at 95°C for 15 s, at 60°C for 60 s, and at 95°C for 15 s. After the reaction, the CT value given by the instrument was analyzed and processed as follows: with GAPDH as the internal reference gene, $\Delta Ct = Ct(\text{target gene}) - CT(\text{GAPDH})$; $\Delta\Delta Ct = \Delta Ct(\text{experimental group}) - \Delta Ct(\text{control group})$; and the relative mRNA expression of target gene = $2^{-\Delta\Delta Ct}$. Primer sequences are shown in Table I.

Western Blot

An amount of 200 µl radio immunoprecipitation assay (RIPA) lysate was added to every 100 mg of tissue; the tissue was repeatedly ground in

ice water until it was uniform without significant lumps; which was then centrifuged at 4°C at 12,000-16,000 g for 5 min; and the supernatant was aspirated to the pre-cooled centrifuge tube, which was the total protein. bicinchoninic acid assay (BCA) solution was added for protein quantification. For electrophoresis after sample loading, the starting voltage was 8 V/cm. When the dye entered the separation gel, the voltage increased to 15 V/cm. The electrophoresis continued until the dye reached the bottom of the separation gel, then the power was disconnected, and the gel was analyzed by Western blot. After the sodium dodecyl sulfate-polyacrylamide gel electrophoresis (SDS-PAGE) electrophoresis, the gel was transferred to polyvinylidene difluoride (PVDF) membrane. The PVDF membrane loaded with protein was quickly put into a sealing buffer (containing 5% skimmed milk powder/bovine serum albumin (BSA)) and incubated in a shaking table at room temperature overnight at 4°C. In the next step, the primary antibodies (ITGB3, p38MAPK/p-p38MAPK, GSK-3 β /p-GSK-3 β , Cx-43/p-Cx43, Bcl-2 and Bax) were diluted with 5% skimmed milk powder/BSA-Tris Buffered Saline-Tween (TBS-T) buffer solution to the working concentration. The membrane was placed in the primary antibody solution and incubated at room temperature at 4°C overnight. After the primary antibody solution was removed, the membrane was washed with TBS-T solution for 3 times, 10 min each; the Horseradish Peroxidase (HRP)-labeled secondary antibody was diluted to the working concentration with 5% skimmed milk powder/BSA-TBS-T buffer solution, and then the membrane was placed in the secondary antibody and incubated in a shaker at 37°C for 1

Table I. Real time PCR primers.

Gene	Primer sequences (5'-3')
ITGB3	Forward: 5'-GGGCCCAACATCTGTACCAC-3', Reverse: 5'-GATGTCCACAGGGTAATCCTCCAC-3'
IL-1	Forward: 5'-ATGGCAACTGTTCCCTGAACTC-3' Reverse: 5'-TTAGGAAGACACGGATTCCAT-3'
IL-6	Forward: 5'-GGCCCTTGCTTTCTCTTCG-3' Reverse: 5'-ATAATAAAGTTTGATTATGT-3'
TNF- α	Forward: 5'-CAGCCTCTTCTCCTCCCTGA-3' Reverse: 5'-GGAAGACCCCTCCCAGATAGA-3'
Bcl-2	Forward: 5'-GACAGAAGATCATGCCGTCC-3' Reverse: 5'-GGTACCAATGGCACTTCAAG-3'
Bax	Forward: 5'-CTGAGCTGACCTTGGAGC-3' Reverse: 5'-GACTCCAGCCACAAAGATG-3'
GAPDH	Forward: 5'-TCTCTGCTCCTCCCTGTTC-3' Reverse: 5'-ACACCGACCTTCACCATCT-3'

h. After the removal of the secondary antibody solution and membrane washing for 3 times, 10 min each, X-ray films were immersed in the fixing solution immediately after exposure and development, with a general fixing time of 5-10 min, until the film was transparent. After washing away the residual fixer with tap water, the slides were dried at room temperature, and the results were observed and photographed after developing in a darkroom. Image J software was used to analyze the gray value of the target band. GAPDH was used as the internal parameter. The ratio of the gray value of the target band to the internal reference band was used as the relative protein expression. This method was also suitable for the detection of Western blot in cells.

Cell Culture

H9c2 cells were cultured in medium containing 10% fetal bovine serum (FBS) at 37°C in CO₂ incubator. The medium was changed every two days, and the cells were passaged every 2-3 days. When the cells of passage 6-7 grew to 70% - 80% confluence, the cells were washed with phosphate-buffered saline (PBS) 24 h before the experiment, and the FBS-free medium was replaced for incubation overnight in the incubator to synchronize the cells and eliminate the influence of serum. The synchronized H9c2 cells were placed into the incubator under hypoxia condition (5% CO₂, 1% O₂, and 94% N₂) for 24 h at 37 °C. The cells were taken out and replaced with medium containing 10% FBS, and cultured at 37 °C for 12 h under reoxygenation conditions (5% CO₂, 21% O₂, and 71% N₂).

Cell Grouping and Transfection According to Different Design Protocol

The day before the experiment, H9c2 cells were taken out for observation to use cells in good growth state for lentivirus transfection. After discarding the original medium, the residual medium was washed twice with PBS buffer solution, and 1 ml of 0.08% trypsin was added and digested in a 5% CO₂ incubator at 37°C for 1 min. After the cells became round under the microscope, digestion was stopped with 2 mL 15% FBS Dulbecco's Modification of Eagle's Medium Dulbecco (DMEM) medium. The wall of the dish was knocked so that the cells fell off the bottom of the dish, and the cell suspension was blown into a single cell suspension with a pipette tip. The single cell suspension was transferred to a 15 ml centrifuge tube, centrifuged at 800 rpm for

5 min at room temperature. The supernatant was discarded and 1 ml of fresh 15% FBS DMEM medium was added to re-suspend the cells. An amount of 50 µL cell suspension was used for counting with a Cell Counting Meter. Cells were seeded into a 6-well plate according to the density of 3×10⁵ cells/well. The cells were cultured overnight in 5% CO₂ incubator at 37°C in 2 mL medium per well. On the day of experiment, when the cell confluence was 30% - 50%, lentiviral transfection could be carried out.

Liposome transfection was performed according to the instructions of Lipofectamine 2000. Cells were divided into the normal group (normal H9c2 cells); SI/R group (H9c2 cells were cultured under normal conditions, and the ischemia/reperfusion injury group was simulated with hypoxia for 24 h and reoxygenation for 12 h; siRNA-NC group (modeling H9c2 cells + transfection of siRNA NC), Anisomycin group (modeling H9c2 cells + MAPK signaling pathway agonist), SB203580 group (modeling H9c2 cells + MAPK signaling pathway inhibitor), ITGB3-siRNA group (modeling H9c2 cells + transfection of ITGB3-siRNA), SB203580 + ITGB3-siRNA group (modeling H9c2 cells + MAPK signaling pathway agonist + transfection of ITGB3-siRNA). The activation or inhibition of MAPK signaling pathway was realized by using Anisomycin or SB203580 for 48 h for agonist or inhibitor treatment, followed by cell transfection.

Transfection of ITGB3-siRNA

Following the operation of the above steps, the transfection of ITGB3-siRNA was described as follows: The transfection could be carried out when the cells reached 50% growth of the 6-well plate. In the step of preparing transfection mixture that was finished in Eppendorf (EP) tube without RNase, 100pmol ITGB3-siRNA (primer sequences of ITGB3: forward primer: CCAGAUCUGGAAGCUCUUTT; reverse primer: AAGAGCUUCCAGGAUCUGGTT; negative control: forward primer: UUCUC-GAACGUGUCACGUTT; reverse primer: AC-GUGACACGUUCGGAGAATT) was added with 250 µl Opti-MEM and mixed with gentle shaking, followed by mixing of the 25 µL Lipo2000 transfection reagent and 250 µL Opti-MEM. The prepared mixture was placed at room temperature for 5 min. After that, the ITGB3-siRNA was mixed with Liposome2000 transfection reagent and incubated at room temperature for 20 min to form the liposome complex. Subsequently,

the medium in the 6-well plate was replaced by DMEM medium without serum and antibiotics. The above mixture was then added into the culture dish and mixed well by shaking the dish back and forth gently. The culture medium was then placed with complete medium after 6 h of culture. Cells were collected after 48 h of culture for subsequent experiment.

3-(4,5)-dimethylthiaziazolo (-z-y1)- 3,5-di-phenyltetrazoliumromide (MTT) Detection of Cell Proliferation

Succinate dehydrogenase in mitochondria of living cells can reduce exogenous MTT to water-insoluble blue violet crystal formazan, which can be deposited in cells, but not in dead cells. Meanwhile, dimethylsulfoxide (DMSO) can dissolve methylzan in living cells. Therefore, the number of living cells can be indirectly reflected by the absorbance value measured at 490 nm. Within a certain range of cell number, the amount of MTT crystal formation is directly proportional to the number of living cells. In this experiment, H9c2 cells were cultured in 96-well cell culture plate, and the density of cells was $1 \times 10^5/\text{ml}$ in each well. A blank control well parallel to the experimental group was set up, which only added culture medium without cells. Six replicates were set for each group. After 48 h of culture in medium containing 10% FBS, the serum-free medium was replaced, and the culture was continued for 24 h. After different interventions of hypoxia/reoxygenation, 20 μL MTT solution (5 mg/ml) was added into the culture medium, and the culture was continued at 37 °C for 4 h, after which the supernatant of the medium was discarded. Then, 150 μL DMSO was added into each well, and the optical density was read at 490 nm of the Microplate Reader. The results were expressed as the survival rate of myocardial cells according to the formula of (absorbance value of experimental group - that of blank control group)/(absorbance value of control group - that of the blank control group) $\times 100\%$.

Flow Cytometry Detection of Cell Apoptosis

Flow cytometry is a single cell quantitative analysis and sorting technique using flow cytometer. DNA fragmentation occurs in apoptotic cells, in which large fragments of DNA can form a distribution area with DNA content less than 2n, which is called "sub-G1 peak". However, this phenomenon is not found in necrotic cells. An-

nexin-V, a calcium dependent phospholipid binding protein, can bind to phosphatidylserine which is reversed to the outer membrane during apoptosis. Using fluorescein isothiocyanate/propidium iodide (FITC) labeled Annexin-V as a fluorescent probe, propidium iodide (PI) nucleic acid embedded dye can be embedded into the double helix structure, so that both DNA and RNA can be stained. Flow cytometry showed normal cells in the lower left quadrant, early apoptotic cells in the right lower quadrant, advanced apoptotic cells and necrotic cells in the upper right quadrant, and damaged cells in the upper left quadrant.

Annexin V-FITC/PI double staining was used to detect apoptosis. Cells were digested with 0.25% trypsin, washed twice with PBS, and the results were observed under inverted microscope after adding trypsin to avoid excessive digestion of cells. It was observed that most of the cells contracted and rounded, and the digestion was terminated rapidly with culture medium containing 10% FBS. After washing twice with PBS, H9c2 cells were collected in centrifuge tube at a speed of 1,000 r/min and centrifuged for 5 min, followed by the absorption of the supernatant. Cells were resuspended with 250 μL buffer solution, and the cell concentration was adjusted to $5 \times 10^5/\text{ml}$. After that, the cell suspension was put into 5 ml flow tube and mixed with 5 μL AnnexinV-FITC and 5 μL PI for 15 min of reaction in the dark. Flow cytometry was used to detect and analyze within 1 h, the average value of three replicates was taken, and the experiment was repeated three times.

Statistical Analysis

SPSS 21.0 (IBM, Armonk, NY, USA) was used for statistical analysis, and the average value \pm standard deviation was used to express the measurement data. One-way analysis of variance was used for comparison among groups, and LSD test was used for pairwise comparison between groups. Chi-square or exact probability chi-square test was used to compare the rates. $p < 0.05$ was used to express the statistical significance of comparison.

Results

Modeling of MIRI

In the model of MIRI, the success rate of operation was 90% with 2 mice died (10%). The main causes of death were injury caused by improper tra-

cheal intubation, left atrial appendage hemorrhage and pneumothorax. All mice in sham operation group survived, with normal food intake and steady increase in body weight. However, mice in the MIRI group showed decreased food intake gradually, and slowly increase or even decrease in the body weight, accompanied by hair shedding, hair scattering, mental depression, and even lower limb edema and shortness of breath in the later stage.

HE Staining, TUNEL Staining and TTC Staining to Reflect the Changes of Myocardial Histopathology, Apoptosis Level and Myocardial Infarction Area in the Two Groups of Mice

Under the light microscope, HE staining of myocardial tissue showed that the myocardial tissue in the sham operation group was light red, blue staining in the nucleus, with the observation of endocardium, myocardial membrane and epicardium as well as complete cardiac structure under low power microscope. Under high power

microscope, myocardial cells with various sections could be observed in the myocardial membrane, and the muscle fiber space was rich in small blood vessels and a small amount of connective tissues (Figure 1A). By comparison, in MIRI group, the myocardial fibers were swollen and dissolved, the arrangement of myocardial filaments was disordered, a large number of vacuoles were produced between myofilaments, and focal necrotic areas were found in myocardium, with the infiltration of a large number of inflammatory cells (Figure 1A).

Furthermore, according to the results of TUNEL staining (Figure 1B), the apoptotic nuclei were brown the normal nuclei were light blue, and the apoptotic nuclei were brown. Only a few apoptotic cells were found in the sham operation group, while the number of apoptotic cells in the MIRI group was significantly increased. The myocardial apoptosis rates of sham operation group and MIRI group were $(9.24 \pm 1.03)\%$ and $(38.77 \pm 3.64)\%$, respectively. Compared with the sham operation group, the number of positive

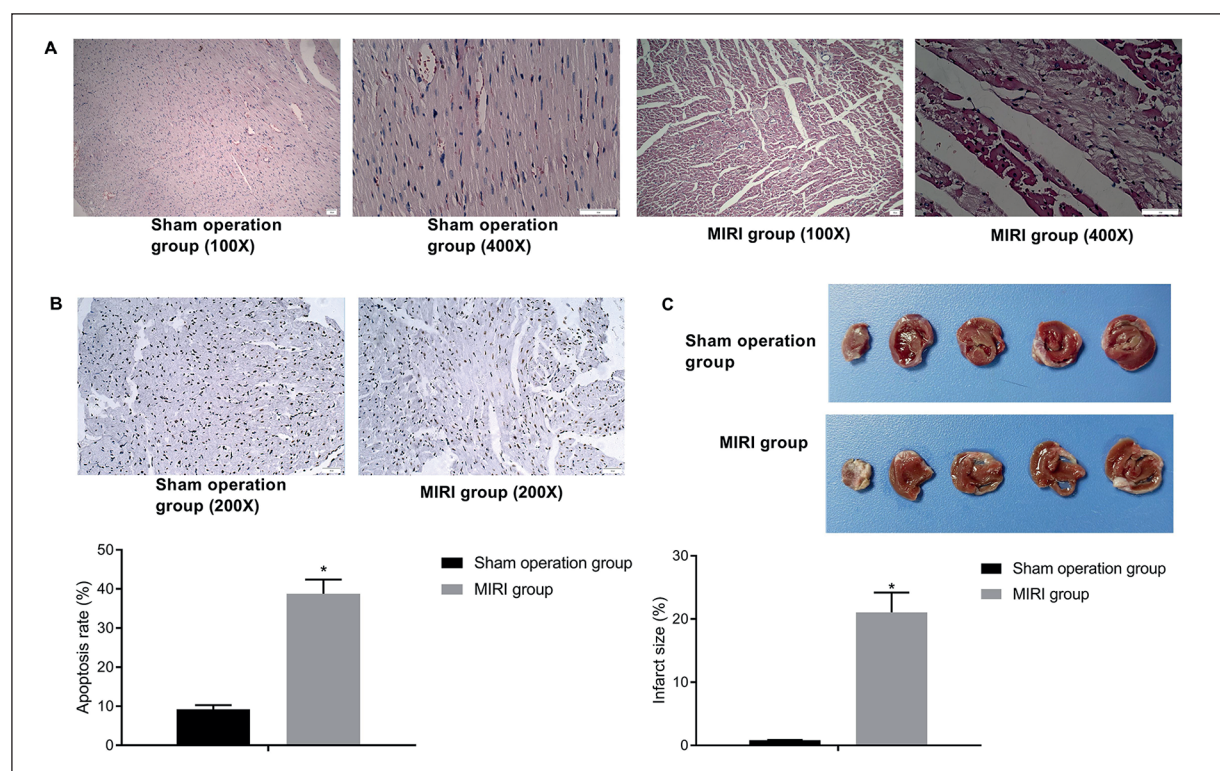


Figure 1. HE staining, TUNEL staining and TTC staining to reflect changes in myocardial histopathology, apoptosis level and myocardial infarction area in the two groups of experimental mice. Note: **A**, HE staining of myocardial tissue of mice in sham operation group and MIRI group (100× and 400×, respectively); **B**, TUNEL staining of myocardial tissue of mice in sham operation group and MIRI group (200×; Top: TUNEL staining; Bottom: Apoptosis rate comparison); **C**, TTC staining of myocardial tissue of mice in sham operation group and MIRI group (Top: TTC staining; Bottom: Infarct size comparison); *Compared with the sham operation group, $p < 0.05$.

cells and the apoptosis rate of MIRI group were significantly increased with statistical difference (Figure 1B, $p < 0.05$).

In addition, TTC staining (Figure 1C) revealed that the normal myocardial tissue was stained red and the infarcted myocardium was stained white. The sham operation group had almost no infarct area, and the infarct size of group MIRI was $(21.05 \pm 3.14)\%$. It was found that the myocardial infarction area was significantly increased in the MIRI group when compared with the sham operation group (Figure 1C, $p < 0.05$).

The mRNA and Protein Expression Levels of Myocardial Tissue-Related Proteins in the Two Groups of Mice

The results of qRT-PCR and Western blot were shown in Figure 2. According to the qRT-PCR results, the expression level of IL-1, IL-6 and TNF- α were significantly upregulated in the MIRI group than that in the sham operation group

(Figure 2A, all $p < 0.05$). Meanwhile, compared with the sham operation group, the mRNA expression of ITGB3 and Bax were significantly increased while that of p38MAPK, GSK-3 β , Cx43 and Bcl-2 was evidently decreased in the MIRI group, showing statistical difference (Figure 2B, all $p < 0.05$). At the same time, at the protein level, ITGB3, and Bax protein expressions were up-regulated while that of p-p38MAPK, p-GSK-3 β , p-Cx43 and Bcl-2 was downregulated in MIRI group than those in the sham operation group (Figure 2C, all $p < 0.05$); while there was no significant change in the expression of p38MAPK, GSK-3 β and Cx43 (all $p > 0.05$).

The mRNA and Protein Expression Levels of Related Proteins in Each Group After Transfection

According to the results of qRT-PCR (Figure 3A), compared with normal group, the mRNA expressions of ITGB3 and Bax were all increased

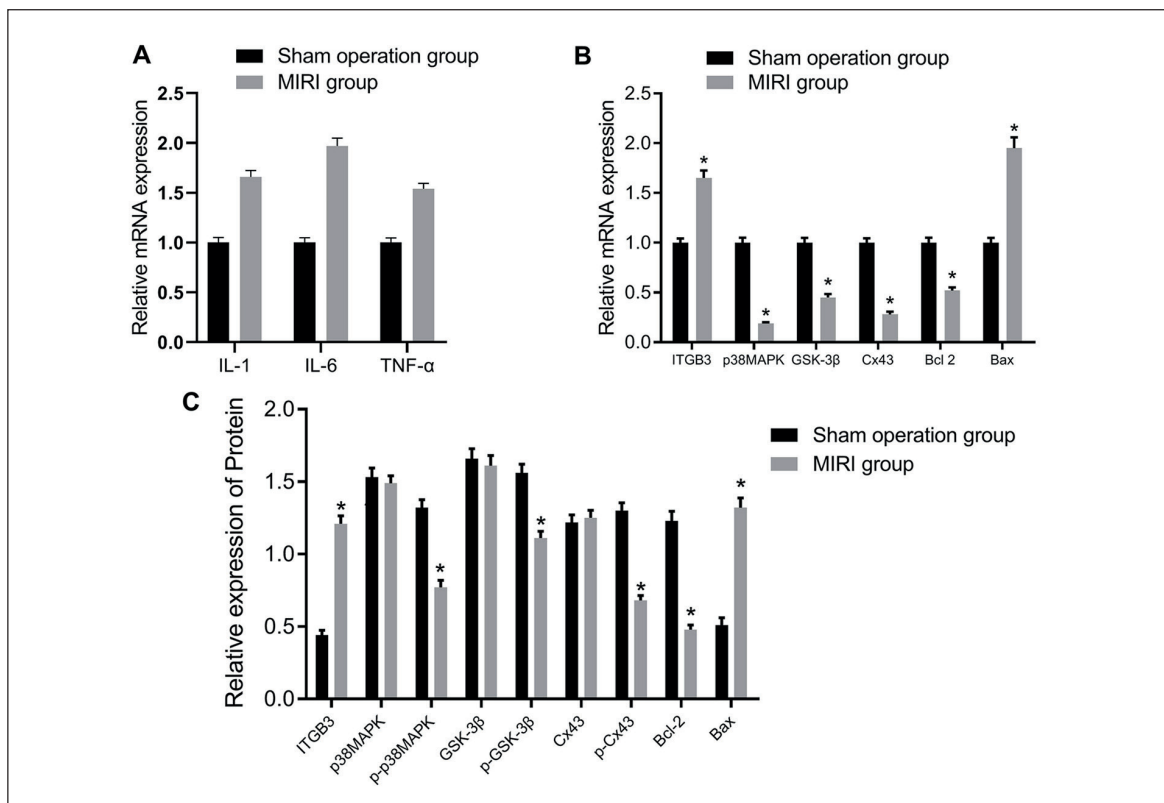


Figure 2. The mRNA and protein expression levels of myocardial tissue-related proteins in the two groups of experimental mice. Note: **A**, The mRNA expression level of IL-1, IL-6 and TNF- α detected by qRT-PCR in myocardial tissue of mice in sham operation group and MIRI group; **B**, The mRNA expression level of ITGB3, p38MAPK, GSK-3 β , Cx43, Bcl-2 and Bax detected by qRT-PCR in myocardial tissue of mice in sham operation group and MIRI group; **C**, The protein expression level of ITGB3, p38MAPK/p-p38MAPK, GSK-3 β /p-GSK-3 β , Cx43/p-Cx43, Bcl-2 and Bax revealed by Western blot in myocardial tissue of mice in sham operation group and MIRI group; *Compared with the shame operation group, $p < 0.05$.

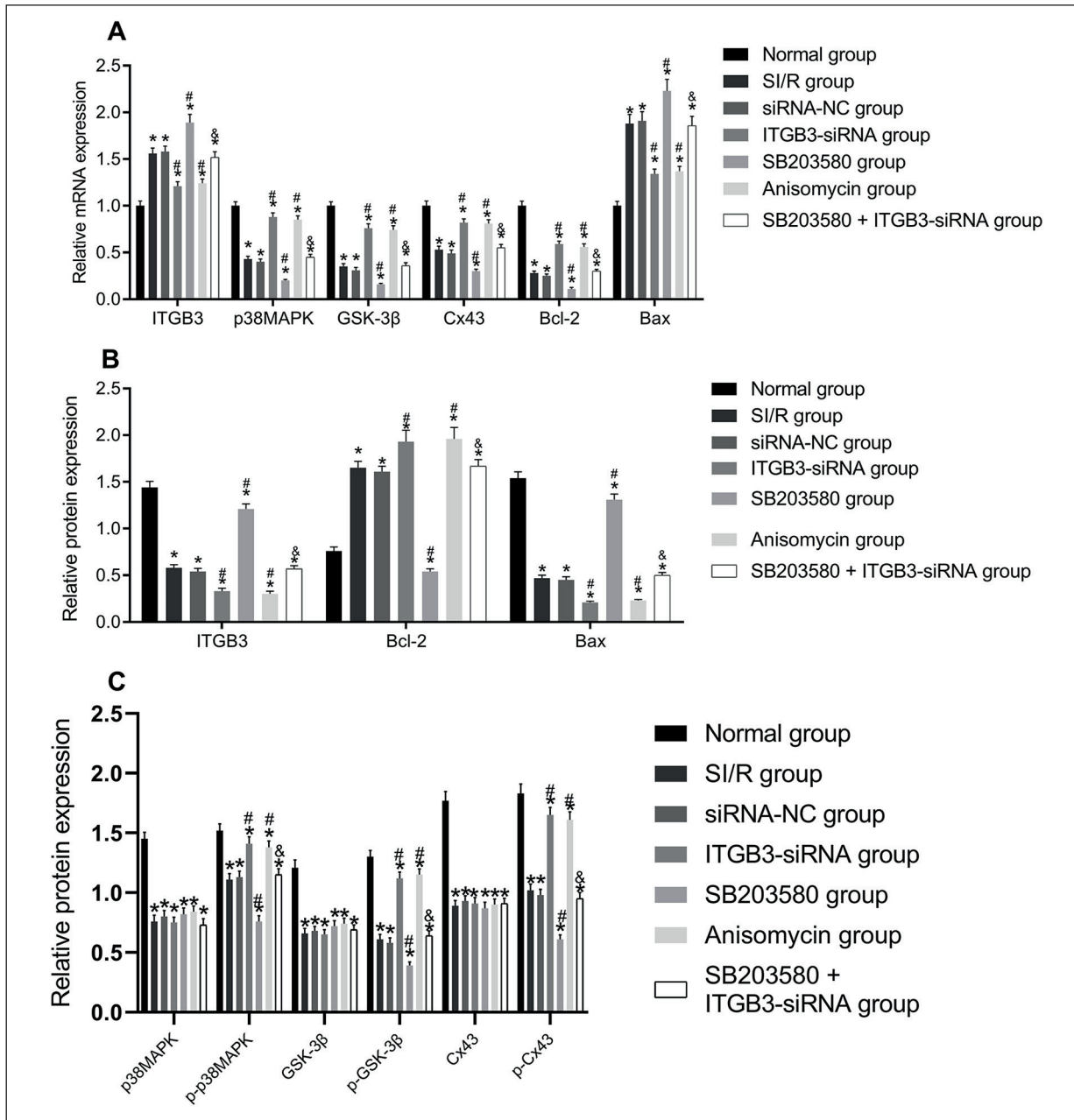


Figure 3. The mRNA and protein expression levels of related proteins in each group after cell transfection. Note: **A**, The mRNA expression level of ITGB3, p38MAPK, GSK-3 β , Cx43, Bcl-2 and Bax detected by qRT-PCR in each group after transfection; **B**, The protein expression level of ITGB3, Bcl-2 and Bax detected by Western blot in each group after transfection; **C**, The protein expression level of p38MAPK/p-p38MAPK, GSK-3 β /p-GSK-3 β and Cx43/p-Cx43 detected by Western blot in each group after transfection; *Compared with Normal group, $p < 0.05$; #Compared with SI/R or siRNA-NC group, $p < 0.05$; &Compared with ITGB3-siRNA group, $p < 0.05$.

while p38MAPK, GSK-3 β , Cx43 and Bcl-2 expression was decreased in the other groups (all $p < 0.05$). There was no statistical difference in the mRNA expression of ITGB3, p38MAPK, GSK-3 β , Cx43, Bax and Bcl-2 between SI/R group and siRNA-NC group (all $p > 0.05$). Furthermore,

compared with siRNA-NC group, ITGB3-siRNA group had markedly decreased mRNA expressions of ITGB3 and Bax, but increased mRNA expression of p38MAPK, GSK-3 β , Cx43 and Bcl-2 (all $p < 0.05$). Furthermore, no significant change was found in the mRNA expres-

sion of ITGB3 in Anisomycin group ($p>0.05$), but p38MAPK, GSK-3 β , Cx43 and Bcl-2 mRNA expressions were highly increased while Bax mRNA expression was evidently decreased in this group (all $p<0.05$). Meanwhile, no significant change of ITGB3 was also found in SB203580 group ($p>0.05$), yet with markedly decreased mRNA expressions of p38MAPK, GSK-3 β , Cx43 and Bcl-2 while significantly increased mRNA expression of Bax (all $p<0.05$). There was no significant difference in mRNA expressions of ITGB3, p38MAPK, GSK-3 β , Cx43, Bax and Bcl-2 between ITGB3-siRNA group and Anisomycin group (all $p>0.05$). Besides, in relative to SI/R group, SB203580 + ITGB3-siRNA group had reduced mRNA expression of ITGB3 ($p<0.05$), but no evident change in the mRNA expression of p38MAPK, GSK-3 β , Cx43, Bax and Bcl-2 (all $p>0.05$). While compared with ITGB3-siRNA group, SB203580 + ITGB3-siRNA group showed no significant difference in the mRNA expression of ITGB3 ($p>0.05$), but there was a significant increase in the mRNA expression of Bax but decrease in p38MAPK, GSK-3 β , Cx43 and Bcl-2 mRNA expression (all $p<0.05$).

Meanwhile, as indicated by the detection results of Western blot (Figure 3B, C): there were statistical differences that the protein expressions of ITGB3 and Bax were increased but p-p38MAPK, p-GSK-3 β , p-Cx43 and Bcl-2 expression was decreased in the other groups (all $p<0.05$), yet there was no significant change in the protein expression of p38MAPK, GSK-3 β and Cx43. No statistical difference was found in the protein expression of ITGB3, p38MAPK/p-p38MAPK, GSK-3 β /p-GSK-3 β , Cx43/p-Cx43, Bcl-2 and Bax between SI/R group and siRNA-NC group (all $p>0.05$). Compared with siRNA-NC group, ITGB3-siRNA group had markedly decreased protein expressions of ITGB3, and Bax but increased protein expression of p-p38MAPK, p-GSK-3 β , p-Cx43 and Bcl-2 (all $p<0.05$), but no significant change in the protein expression of p38MAPK, GSK-3 β and Cx43 (all $p>0.05$). Both Anisomycin group and SB203580 group had no significant change in the protein expression of ITGB3 ($p>0.05$), while Anisomycin group had evidently increased protein expressions of p-p38MAPK, p-GSK-3 β , p-Cx43 and Bcl-2 but decreased protein expression of Bax (all $p<0.05$); and an opposite trend was found in SB203580 group (all $p<0.05$); but no change in p38MAPK, GSK-3 β and Cx43 (all $p>0.05$). No significant difference was found between ITGB3-siRNA group and Anisomycin

group ($p>0.05$). In addition, compared with SI/R group, SB203580 + ITGB3-siRNA group had decreased expression of ITGB3 ($p<0.05$), while there was no difference in the protein expression of p38MAPK/p-p38MAPK, GSK-3 β /p-GSK-3 β , Cx43/p-Cx43, Bcl-2 and Bax (all $p>0.05$). Moreover, compared with ITGB3-siRNA group, SB203580 + ITGB3-siRNA group had no significant change in ITGB3, p38MAPK, GSK-3 β and Cx43 (all $p>0.05$), but showed significant upregulation in the protein expression of Bax, while downregulation in that of p-p38MAPK, p-GSK-3 β , p-Cx43 and Bcl-2 (all $p<0.05$).

Cell Proliferation in Each Group After Transfection

In view of cell activities by using MTT assay (Figure 4), there was no significant change in cell proliferation rate at 24 h in all groups (all $p>0.05$). Compared with that at 24 h, the cell proliferation rate 48 h and 72 h had significant difference (all $p<0.05$). Compared with the normal group, the proliferation rate of other groups was decreased (all $p<0.05$). SI/R group and siRNA-NC group showed no significant difference in cell proliferation rate at all time points ($p>0.05$). In relative to SI/R group and siRNA-NC group, ITGB3-siRNA group and Anisomycin group had signifi-

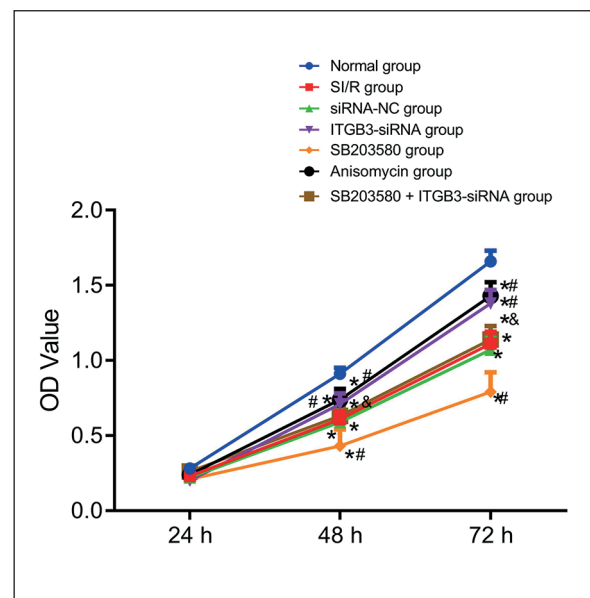


Figure 4. Cell proliferation detected by using MTT assay in each group after cell transfection. Note: *Compared with Normal group, $p<0.05$; #Compared with SI/R or siRNA-NC group, $p<0.05$; &Compared with ITGB3-siRNA group, $p<0.05$.

cantly increased OD values at 48 h and 72 h (all $p < 0.05$); while SB203580 group had significantly decreased OD value at 48 h and 72 h (all $p < 0.05$); but no significant change was found in SB203580 + ITGB3-siRNA group (all $p > 0.05$). Meanwhile, there was no difference in cell proliferation rate between ITGB3-siRNA group and Anisomycin group ($p > 0.05$). In addition, significant change was found in OD values at 48 h and 72 h between SB203580 + ITGB3-siRNA group when compared with ITGB3-siRNA (all $p < 0.05$).

Cell Apoptosis in Each Group After Transfection

As revealed by the results detected using flow cytometry (Figure 5), there was a significantly increase in the apoptosis rate in other groups when compared with the normal group

(all $p < 0.05$). No evident difference was found between SI/R group and siRNA-NC group ($p > 0.05$). Furthermore, compared with siRNA-NC group, ITGB3-siRNA group and Anisomycin group showed reduced cell apoptosis rate (both $p < 0.05$); SB203580 group had increased cell apoptosis rate ($p < 0.05$); while no statistical difference was found in cell apoptosis rate in SB203580 + ITGB3-siRNA group ($p > 0.05$). Meanwhile, no significant statistical difference in the rate was found between ITGB3-siRNA group and Anisomycin group ($p > 0.05$). While compared with ITGB3-siRNA group, SB203580 + ITGB3-siRNA group indicated an increased cell apoptosis rate ($p < 0.05$). It suggests that silencing ITGB3 gene expression may inhibit myocardial cell apoptosis through inhibiting the activation of MAPK signaling pathway.

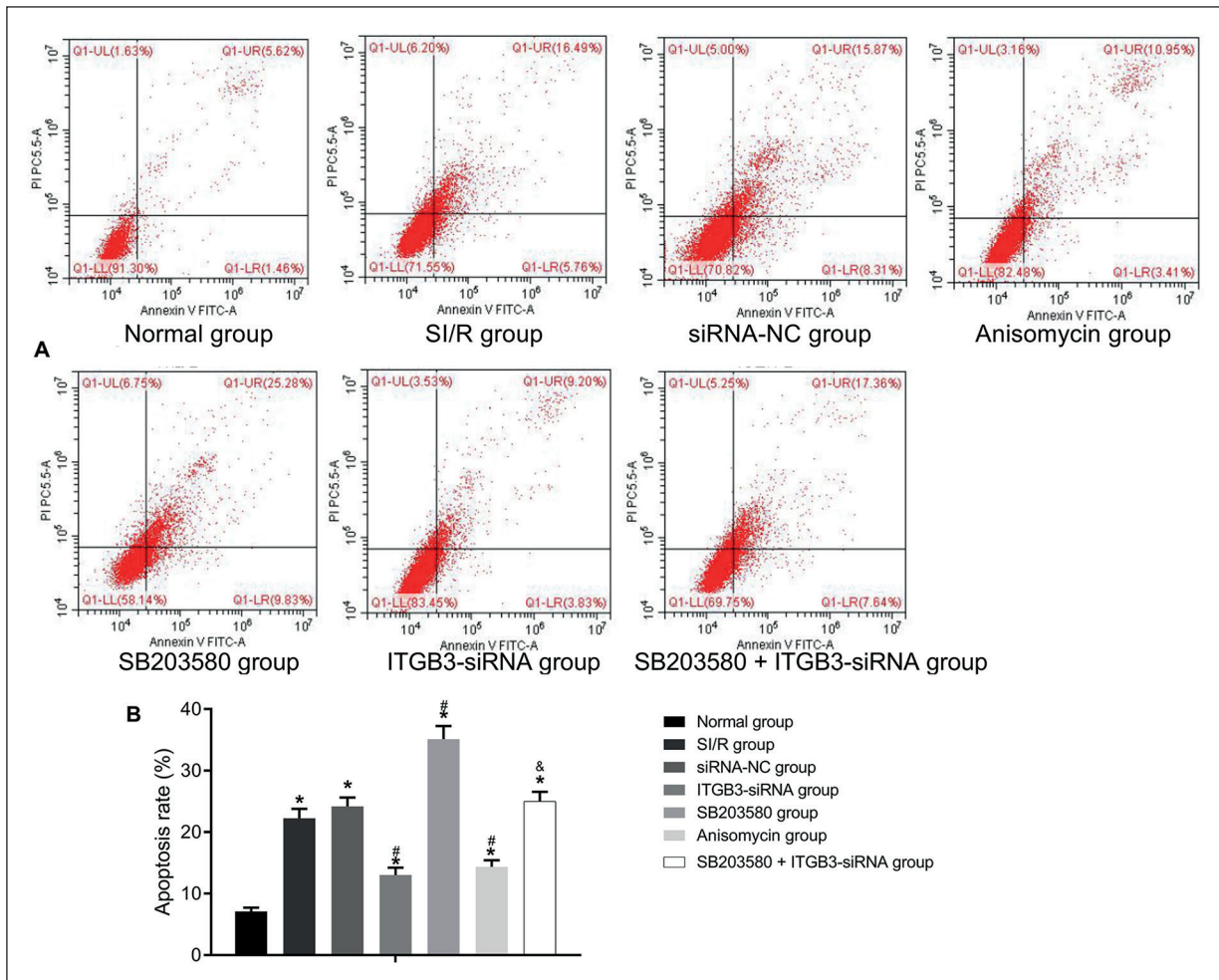


Figure 5. Cell apoptosis detected by using flow cytometry in each group after cell transfection. Note: **A**, Cell apoptosis detected by flow cytometry; **B**, Comparison of cell apoptosis rate in each group; *Compared with Normal group, $p < 0.05$; #Compared with SI/R or siRNA-NC group, $p < 0.05$; &Compared with ITGB3-siRNA group, $p < 0.05$.

The Expression Levels of IL-1, IL-6 and TNF- α in Each Group After Transfection

For another detection of cell IL-1, IL-6 and TNF- α mRNA levels after cell transfection in each group (Figure 6), it was found that compared with Control group, these levels were highly increased in the other groups (all $p < 0.05$). No significant difference was found among SI/R group, siRNA-NC group and SB203580 + ITGB3-siRNA group, or between Anisomycin group and ITGB3-siRNA group. While a significant downregulated trend of IL-1, IL-6 and TNF- α mRNA levels was found in Anisomycin group and ITGB3-siRNA group, and a significant upregulated trend was observed in SB203580 group ($p < 0.05$). Moreover, compared with ITGB3-siRNA group, SB203580 + ITGB3-siRNA had an evidently increase in IL-1, IL-6 and TNF- α mRNA levels, with statistical difference (all $p < 0.05$).

Discussion

Myocardial hypoxia in coronary artery diseases can cause myocardial cell apoptosis, induce inflammatory reaction, further induce myocardial cell loss greatly, and hence result in myocardial remodeling and the occurrence of chronic heart failure³⁵. Therefore, it is of great significance to understand pathways leading to the above-mentioned process and determine possible strategies

to regulate this process. Integrins play a major role in the bidirectional regulation of apoptosis and proliferation³⁶, yet with unclear specific mechanism, especially in vascular cells, and few studies in myocardial cells. This project suggested that ITGB3 inhibits MIRI myocardial cell apoptosis and inflammation by mediating MAPK signaling pathway and studied the role of ITGB3 in MIRI and the possible mechanism of action, so as to provide a new and effective target for MIRI intervention in the future.

MIRI has always been a hot topic in medical field³⁷. At present, it is believed that the pathological mechanism of ischemia-reperfusion injury may be related to various factors, such as excessive generation of oxygen free radicals; calcium overload; cytokine participation; accumulation of neutrophils in Kupffer cell activator; energy depletion of stem cells; imbalance of endothelin and nitric oxide concentration; excessive release of inflammatory mediators, etc.^{38,39}. Concerning MAPK pathway, a large number of oxygen free radicals and cytokines can be released during reperfusion that may result in the activation of MAPK signaling pathway. MAPK may further mediate the expression of various transcription factors, and be involved in the process of inflammation, metabolic disorder and cell apoptosis⁴⁰. Specifically, MAPK protein family has been reported to have the ability to activate phosphorylation downstream functional proteins and participate in the regulation of cell division, apop-

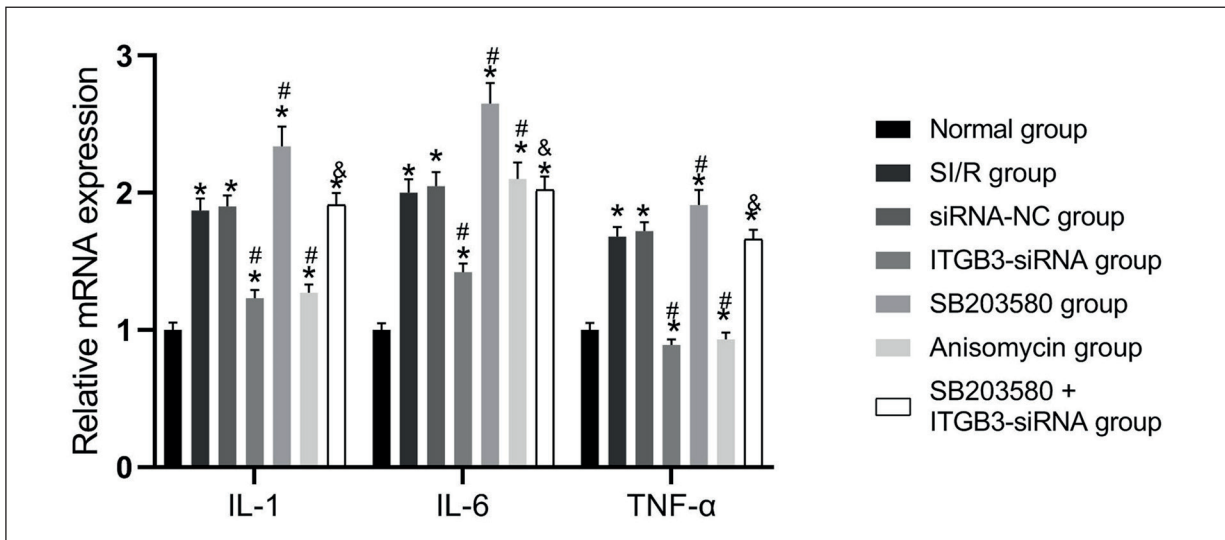


Figure 6. The expression level of IL-1, IL-6 and TNF- α detected by qRT-PCR in each group after cell transfection. Note: *Compared with Normal group, $p < 0.05$; #Compared with SI/R or siRNA-NC group, $p < 0.05$; &Compared with ITGB3-siRNA group, $p < 0.05$.

tosis, metabolism, and differentiation gene and protein expression⁴¹. Its members consist of c-Jun N-terminal kinase (JNK), extracellular regulated protein kinase (ERK) and p38 protein kinase, all of which function significantly in many cell events⁴². In addition, the powerful role of ITGB3 has been introduced in our study. At the same time, previous studies have reported that ITGB3 plays a role in the occurrence and development of myocardial cell apoptosis^{43,44}; and there are also individual reports that ITGB3 plays an inhibitory role in the process of myocardial cell apoptosis^{45,46}. Besides, dysfunction of integrin can lead to integrin-mediated intercellular connectivity, and then lead to abnormal myocardial contractile dysfunction and arrhythmia⁴⁶.

In our study, the expression of ITGB3 in myocardial tissue of MIRI mice was significantly higher than that of mice received sham operation. It may suggest that downregulated expression of ITGB3 may produce a protective role for myocardial cell injury. Besides, tissue detection also showed that the apoptosis rate in MIRI modeling mouse was significantly increased, accompanied by increased expression of inflammatory indexes IL-1, IL-6 and TNF- α , and enlarged myocardial infarction area. It indicates the presence of apoptosis, inflammation and myocardial infarction during MIRI. There is a need to search for potential approaches to prevent the above events. Importantly, after cell transfection, silencing of ITGB3 expression and Anisomycin treatment both resulted in the increased expressions of p38MAPK/p-p38MAPK, GSK-3 β /p-GSK-3 β , Cx43/p-Cx43 and Bcl-2, but decreased expression of Bax, IL-1, IL-6 and TNF- α ; while the opposite trends of decreased expressions of p38MAPK/p-p38MAPK, GSK-3 β /p-GSK-3 β , Cx43/p-Cx43 and Bcl-2, and increased expression of Bax, IL-1, IL-6 and TNF- α were found after SB203580 treatment. It may inspire our researcher that silencing of ITGB3 expression may have a myocardial protection through the elevation of phosphorylation of p38MAPK, GSK-3 β and Cx43 to promote the activation of MAPK signaling pathway and through the suppression of inflammatory reaction. Meanwhile, simultaneous experiments on myocardial cell proliferation and cell apoptosis verified that silencing of ITGB3 expression and Anisomycin treatment could both promote cell proliferation while suppress cell apoptosis. However, the beneficial role of ITGB3 expression silencing was reversed by SB203580

treatment, which in turn proves the positive role of ITGB3 gene expression silencing and the potential interaction between ITGB3 and MAPK signaling pathway.

As for the mechanism, it is speculated by our researcher that silenced expression of ITGB3 promoted the activation of MAPK signaling pathway, which further induce the increased phosphorylated levels of p38MAPK, GSK-3 β and Cx43, that is, the decreased activities. The phosphorylated p38MAPK, GSK-3 β and Cx43 can interact with adenine nucleotide translocation enzyme in mitochondrial intima, reducing the opening of mitochondrial permeability transition pore and inhibiting cell apoptosis^{47,48}. Besides, the above process can also help to activate mitochondrial ATP sensitive potassium channel and inhibit myocardial cell apoptosis⁴⁹. Myocardial cell apoptosis plays a key role in cardiac remodeling and heart failure after myocardial infarction. Inhibition of myocardial cell apoptosis can effectively improve cardiac function and left ventricular remodeling after myocardial infarction. Sudden blockage of coronary artery causes myocardial ischemia, and thus produces irreversible injury and necrosis of myocardial cells⁵⁰. The content released by the necrotic cells after rupture activated the autoimmune system, resulting in the release of cell membrane components in mitochondria and the activation of complement in the complement cascade reaction, thus triggering serious inflammatory reaction⁵¹. Subsequently, neutrophils and macrophages are recruited to eliminate the debris and matrix of dead cells. It shall be noted that the release of inflammatory mediators on the one hand initiates the repair of myocardial tissue, which plays an important role in the process of myocardial healing after acute ischemia⁵². On the other hand, however, excessive inflammatory response will lead to matrix degradation and myocardial cell death, and increase the degree of primary myocardial injury. Our study for the first clarifies that silenced expression of ITGB3 works in coordination with the activation of MAPK signaling pathway to prevent myocardial cell apoptosis and promote cell proliferation through the impact on the downstream GSK-3 β and Cx43 pathways as well as suppressed inflammatory mediators.

So far, no suitable drug or bioactive substance has been found to achieve cardiac protection strategy. Ischemic postconditioning as an endogenous defense mechanism has attracted wide attention, but its clinical application generates

no significant outcome. Gene silencing mediated signaling pathway can simulate and explore the methods of molecular targeted therapy on myocardial protection, which has a good application prospect. Our study agrees and supports the value of gene therapy in the treatment of human disorders. More significantly, our study constructed two experimental models of mice with MIRI and cell transfection in myocardial cells. Based on the technique of gene silencing and reasonable hypothesis, our study explored and explained the role and mechanism of ITGB and MAPK in cell proliferation, apoptosis and inflammation successfully. Of course, there are also some shortcomings in this study. Firstly, although H9c2 cells have been widely used in cardiovascular research, they may not be able to accurately represent the response of normal myocardial cells to exogenous intervention. Secondly, this investigation did not confirm the role of the proposed signaling axis in myocardial protection. Simultaneously, we only detected the reaction of some inflammatory factors, and did not involve other inflammatory factors as well as signal pathway related to inflammation, which need further in-depth study.

Conclusions

To sum up, silencing ITGB3 gene expression can inhibit the activation of MAPK signaling pathway, regulate the downstream GSK-3 β and Cx43 signaling pathways, promote the proliferation of mouse myocardial cells, inhibit myocardial cell apoptosis and inflammatory reaction, and thus have protective effect on MIRI in mice. Our study may provide a new insight in understanding the pathogenesis of MIRI and inspire researchers to formulate updated therapeutic approaches for the treatment of MIRI from a perspective of molecular therapy.

Conflict of Interest

The Authors declare that they have no conflict of interests.

References

- 1) Kraushaar LE, Krämer A. Are we losing the battle against cardiometabolic disease? The case for a paradigm shift in primary prevention. *BMC Public Health* 2009; 9: 64.
- 2) Zhou T, Chuang CC, Zuo L. Molecular Characterization of Reactive Oxygen Species in Myocardial Ischemia-Reperfusion Injury. *Biomed Res Int* 2015; 2015: 864946.
- 3) Yuan L, Dai X, Fu H, Sui D, Lin L, Yang L, Zha P, Wang X, Gong G. Vaspin protects rats against myocardial ischemia/reperfusion injury (MIRI) through the TLR4/NF- κ B signaling pathway. *Eur J Pharmacol* 2018; 835: 132-139.
- 4) Shen Y, Liu X, Shi J, Wu X. Involvement of Nrf2 in myocardial ischemia and reperfusion injury. *Int J Biol Macromol* 2019; 125: 496-502.
- 5) Aghaei M, Motallebnezhad M, Ghorghanlu S, Jabbari A, Enayati A, Rajaei M, Pourabouk M, Moradi A, Alizadeh AM, Khori V. Targeting autophagy in cardiac ischemia/reperfusion injury: A novel therapeutic strategy. *J Cell Physiol* 2019; 234: 16768-16778.
- 6) Xia Z, Li H, Irwin MG. Myocardial ischaemia reperfusion injury: the challenge of translating ischaemic and anaesthetic protection from animal models to humans. *Br J Anaesth* 2016; 117 Suppl 2: ii44-ii62.
- 7) Kannan S, Boovarahan SR, Rengaraju J, Prem P, Kurian GA. Attenuation of cardiac ischemia-reperfusion injury by sodium thiosulfate is partially dependent on the effect of cystathione beta synthase in the myocardium. *Cell Biochem Biophys* 2019; 77: 261-272.
- 8) Nandi S, Ravindran S, Kurian GA. Role of endogenous hydrogen sulfide in cardiac mitochondrial preservation during ischemia reperfusion injury. *Biomed Pharmacother* 2018; 97: 271-279.
- 9) Wang EW, Han YY, Jia XS. PAFR-deficiency alleviates myocardial ischemia/reperfusion injury in mice via suppressing inflammation, oxidative stress and apoptosis. *Biochem Biophys Res Commun* 2018; 495: 2475-2481.
- 10) Chang X, Zhang K, Zhou R, Luo F, Zhu L, Gao J, He H, Wei T, Yan T, Ma C. Cardioprotective effects of salidroside on myocardial ischemia-reperfusion injury in coronary artery occlusion-induced rats and Langendorff-perfused rat hearts. *Int J Cardiol* 2016; 215: 532-544.
- 11) Techiryan G, Weil BR, Palka BA, Canty JM Jr. Effect of Intracoronary Metformin on Myocardial Infarct Size in Swine. *Circ Res* 2018; 123: 986-995.
- 12) Sachdeva J, Dai W, Gerczuk PZ, Kloner RA. Combined remote preconditioning and postconditioning failed to attenuate infarct size and contractile dysfunction in a rat model of coronary artery occlusion. *J Cardiovasc Pharmacol Ther* 2014; 19: 567-573.
- 13) Balakumar P, Rohilla A, Singh M. Pre-conditioning and postconditioning to limit ischemia-reperfusion-induced myocardial injury: what could be the next footstep?. *Pharmacol Res* 2008; 57: 403-412.
- 14) Kunecki M, Płazak W, Roleder T, Biernat J, Oleksy T, Podolec P, Gołba KS. 'Opioidergic post-conditioning' of heart muscle during ischemia/reperfusion injury. *Cardiol J* 2017; 24: 419-426.

- 15) Peng B, Guo QL, He ZJ, Ye Z, Yuan YJ, Wang N, Zhou J. Remote ischemic postconditioning protects the brain from global cerebral ischemia/reperfusion injury by up-regulating endothelial nitric oxide synthase through the PI3K/Akt pathway. *Brain Res* 2012; 1445: 92-102.
- 16) Shi J, Guan J, Jiang B, Brenner DA, Del Monte F, Ward JE, Connors LH, Sawyer DB, Semigran MJ, Macgillivray TE, Seldin DC, Falk R, Liao R. Amyloidogenic light chains induce cardiomyocyte contractile dysfunction and apoptosis via a non-canonical p38alpha MAPK pathway. *Proc Natl Acad Sci U S A* 2010; 107: 4188-4193.
- 17) Topolska-Woś AM, Rosińska S, Filipek A. MAP kinase p38 is a novel target of CacyBP/SIP phosphatase. *Amino Acids* 2017; 49: 1069-1076.
- 18) Nishioka C, Ikezoe T, Yang J, Yokoyama A. Tetraspanin Family Member, CD82, Regulates Expression of EZH2 via Inactivation of p38 MAPK Signaling in Leukemia Cells. *PLoS One* 2015; 10: e0125017.
- 19) Cao Q, Karthikeyan A, Dheen ST, Kaur C, Ling EA. Production of proinflammatory mediators in activated microglia is synergistically regulated by Notch-1, glycogen synthase kinase (GSK-3 β) and NF- κ B/p65 signalling. *PLoS One* 2017; 12: e0186764.
- 20) Wang H, Huang S, Yan K, Fang X, Abussaud A, Martinez A, Sun HS, Feng ZP. Tideglusib, a chemical inhibitor of GSK3 β , attenuates hypoxic-ischemic brain injury in neonatal mice. *Biochim Biophys Acta* 2016; 1860: 2076-2085.
- 21) Sharma AK, Kumar A, Sahu M, Sharma G, Datusalia AK, Rajput SK. Exercise preconditioning and low dose copper nanoparticles exhibits cardioprotection through targeting GSK-3 β phosphorylation in ischemia/reperfusion induced myocardial infarction. *Microvasc Res* 2018; 120: 59-66.
- 22) Sulaiman D, Li J, Devarajan A, Cunningham CM, Li M, Fishbein GA, Fogelman AM, Eghbali M, Reddy ST. Paraoxonase 2 protects against acute myocardial ischemia-reperfusion injury by modulating mitochondrial function and oxidative stress via the PI3K/Akt/GSK-3 β RISK pathway. *J Mol Cell Cardiol* 2019; 129: 154-164.
- 23) Mahajan UB, Chandrayan G, Patil CR, Arya DS, Suchal K, Agrawal Y, Ojha S, Goyal SN. Eplerenone attenuates myocardial infarction in diabetic rats via modulation of the PI3K-Akt pathway and phosphorylation of GSK-3 β . *Am J Transl Res* 2018; 10: 2810-2821.
- 24) Macquart C, Jüttner R, Morales Rodriguez B, Le Dour C, Lefebvre F, Chatzifrangkeskou M, Schmitt A, Gotthardt M, Bonne G, Muchir A. Microtubule cytoskeleton regulates Connexin 43 localization and cardiac conduction in cardiomyopathy caused by mutation in A-type lamins gene. *Hum Mol Genet* 2019; 28: 4043-4052.
- 25) Orellana JA, Martinez AD, Retamal MA. Gap junction channels and hemichannels in the CNS: regulation by signaling molecules. *Neuropharmacology* 2013; 75: 567-582.
- 26) Rong B, Xie F, Sun T, Hao L, Lin MJ, Zhong JQ. Nitric oxide, PKC- ϵ , and connexin43 are crucial for ischemic preconditioning-induced chemical gap junction uncoupling. *Oncotarget* 2016; 7: 69243-69255.
- 27) Wang M, Smith K, Yu Q, Miller C, Singh K, Sen CK. Mitochondrial connexin 43 in sex-dependent myocardial responses and estrogen-mediated cardiac protection following acute ischemia/reperfusion injury. *Basic Res Cardiol* 2019; 115: 1.
- 28) Chen X, Yu Y, Mi LZ, Walz T, Springer TA. Molecular basis for complement recognition by integrin α X β 2. *Proc Natl Acad Sci U S A* 2012; 109: 4586-4591.
- 29) Takada Y, Ye X, Simon S. The integrins. *Genome Biol* 2007; 8: 215.
- 30) Traister A, Walsh M, Aafaqi S, Lu M, Dai X, Henkleman MR, Momen A, Zhou YQ, Husain M, Arab S, Piran S, Hannigan G, Coles JG. Mutation in integrin-linked kinase (ILK(R211A)) and heat-shock protein 70 comprise a broadly cardioprotective complex. *PLoS One* 2013; 8: e77331.
- 31) Rapisarda V, Borghesan M, Miguela V, Encheva V, Snijders AP, Lujambio A, O'Loughlen A. Integrin Beta 3 Regulates Cellular Senescence by Activating the TGF- β Pathway. *Cell Rep* 2017; 18: 2480-2493.
- 32) Dong X, Hudson NE, Lu C, Springer TA. Structural determinants of integrin β -subunit specificity for latent TGF- β . *Nat Struct Mol Biol* 2014; 21: 1091-1096.
- 33) Xia ZJ, Hu W, Wang YB, Zhou K, Sun GJ. Expression heterogeneity research of ITGB3 and BCL-2 in lung adenocarcinoma tissue and adenocarcinoma cell line. *Asian Pac J Trop Med* 2014; 7: 473-477.
- 34) Singh AS, Chandra R, Guhathakurta S, Sinha S, Chatterjee A, Ahmed S, Ghosh S, Rajamma U. Genetic association and gene-gene interaction analyses suggest likely involvement of ITGB3 and TPH2 with autism spectrum disorder (ASD) in the Indian population. *Prog Neuropsychopharmacol Biol Psychiatry* 2013; 45: 131-143.
- 35) Yao L, Chen H, Wu Q, Xie K. Hydrogen-rich saline alleviates inflammation and apoptosis in myocardial I/R injury via PINK-mediated autophagy. *Int J Mol Med* 2019; 44: 1048-1062.
- 36) Vellon L, Menendez JA, Lupu R. A bidirectional "alpha(v)beta(3) integrin-ERK1/ERK2 MAPK" connection regulates the proliferation of breast cancer cells. *Mol Carcinog* 2006; 45: 795-804.
- 37) Russo I, Penna C, Musso T, Popara J, Alloatti G, Cavalot F, Pagliaro P. Platelets, diabetes and myocardial ischemia/reperfusion injury. *Cardiovasc Diabetol* 2017; 16: 71.
- 38) Wu MY, Yiang GT, Liao WT, Tsai AP, Cheng YL, Cheng PW, Li CY, Li CJ. Current Mechanistic Concepts in Ischemia and Reperfusion Injury. *Cell Physiol Biochem* 2018; 46: 1650-1667.

- 39) Minutoli L, Puzzolo D, Rinaldi M, Irrera N, Marini H, Arcoraci V, Bitto A, Crea G, Pisani A, Squadrito F, Trichilo V, Bruschetta D, Micali A, Altavilla D. ROS-Mediated NLRP3 Inflammasome Activation in Brain, Heart, Kidney, and Testis Ischemia/Reperfusion Injury. *Oxid Med Cell Longev* 2016; 2016: 2183026.
- 40) Kim EK, Choi EJ. Compromised MAPK signaling in human diseases: an update. *Arch Toxicol* 2015; 89: 867-882.
- 41) Xu XF, Liu F, Xin JQ, Fan JW, Wu N, Zhu LJ, Duan LF, Li YY, Zhang H. Respective roles of the mitogen-activated protein kinase (MAPK) family members in pancreatic stellate cell activation induced by transforming growth factor- β 1 (TGF- β 1). *Biochem Biophys Res Commun* 2018; 501: 365-373.
- 42) Kim HY, Park SY, Choung SY. Enhancing effects of myricetin on the osteogenic differentiation of human periodontal ligament stem cells via BMP-2/Smad and ERK/JNK/p38 mitogen-activated protein kinase signaling pathway. *Eur J Pharmacol* 2018; 834: 84-91.
- 43) Wu J, Zheng C, Wang X, Yun S, Zhao Y, Liu L, Lu Y, Ye Y, Zhu X, Zhang C, Shi S, Liu Z. MicroRNA-30 family members regulate calcium/calci-neurin signaling in podocytes. *J Clin Invest* 2015; 125: 4091-4106.
- 44) Suryakumar G, Kasiganesan H, Balasubramanian S, Kuppuswamy D. Lack of β 3 integrin signaling contributes to calpain-mediated myocardial cell loss in pressure-overloaded myocardium. *J Cardiovasc Pharmacol* 2010; 55: 567-573.
- 45) Su Y, Tian H, Wei L, Fu G, Sun T. Integrin β 3 inhibits hypoxia-induced apoptosis in cardiomyocytes. *Acta Biochim Biophys Sin (Shanghai)* 2018; 50: 658-665.
- 46) Wei L, Zhou Q, Tian H, Su Y, Fu GH, Sun T. Integrin β 3 promotes cardiomyocyte proliferation and attenuates hypoxia-induced apoptosis via regulating the PTEN/Akt/mTOR and ERK1/2 pathways. *Int J Biol Sci* 2020; 16: 644-654.
- 47) Terashima Y, Sato T, Yano T, Maas O, Itoh T, Miki T, Tanno M, Kuno A, Shimamoto K, Miura T. Roles of phospho-GSK-3 β in myocardial protection afforded by activation of the mitochondrial K ATP channel. *J Mol Cell Cardiol* 2010; 49: 762-770.
- 48) Ishikawa S, Kuno A, Tanno M, Miki T, Kouzu H, Itoh T, Sato T, Sunaga D, Murase H, Miura T. Role of connexin-43 in protective PI3K-Akt-GSK-3 β signaling in cardiomyocytes. *Am J Physiol Heart Circ Physiol* 2012; 302: H2536-H2544.
- 49) Rottlaender D, Boengler K, Wolny M, Schwaiger A, Motloch LJ, Ovize M, Schulz R, Heusch G, Hoppe UC. Glycogen synthase kinase 3 β transfers cytoprotective signaling through connexin 43 onto mitochondrial ATP-sensitive K⁺ channels. *Proc Natl Acad Sci U S A* 2012; 109: 21552.
- 50) Groehler A 4th, Kren S, Li Q, Robledo-Villafane M, Schmidt J, Garry M, Tretyakova N. Oxidative cross-linking of proteins to DNA following ischemia-reperfusion injury. *Free Radic Biol Med* 2018; 120: 89-101.
- 51) van der Pals J, Koul S, Andersson P, Götberg M, Ubachs JF, Kanski M, Arheden H, Olivecrona GK, Larsson B, Erlinge D. Treatment with the C5a receptor antagonist ADC-1004 reduces myocardial infarction in a porcine ischemia-reperfusion model. *BMC Cardiovasc Disord* 2010; 10: 45.
- 52) Frangogiannis NG. The inflammatory response in myocardial injury, repair, and remodeling. *Nat Rev Cardiol* 2014; 11: 255-265.